

2D finite-difference modeling and imaging of viscoacoustic wave propagation using a PML absorbing boundary condition

Ali Fathalian and Kris Innanen

ABSTRACT

The constant-Q wave propagation by series of standard linear solid mechanisms using perfectly matched layers absorbing boundary condition (PML) are investigated. An PML with an unsplit field is derived for the viscoacoustic wave equation by introducing the auxiliary variables and their associated partial differential equations. The unsplit PML are tested on a homogeneous velocity and Marmousi velocity models by applying the 2-4 staggered grid finite-difference scheme. When the wave propagating in the subsurface the amplitude and phase of seismic wave distort due to attenuation. The acoustic reverse time migration (RTM) can not explain this distortion, so we used an unsplit viscoacoustic wave equation with constant Q-model. Comparing the numerical tests on synthetic data for unsplit viscoacoustic reverse time migration and acoustic reverse time migration show the advantages of our approach over acoustic RTM when the recorded data had strong attenuation effects.

INTRODUCTION

Absorbing boundary conditions (ABCs) are used in numerical simulations of wave propagation in unbounded problems. To absorb outgoing waves, the reflections from the outer boundary of the computational domain, the ABCs are in finite difference method. There are a number of ABCs for use in finite-difference modeling of acoustic and elastic wave propagation. A lossy material layer to attenuate fields near the computational boundary is used by Cerjan et al. (Cerjan et al., 1985) and Levander (Levander, 1985). The ABCs of Clayton and Engquist (Clayton and Engquist, 1977) introduce an approach based on a paraxial approximation of the elastic wave equation. Although these ABCs successful in many applications, but they adsorb wave imperfectly and the artificial reflections occur at the edges of the computational domain. The perfectly matched layer (PML) introduced by Berenger (Berenger, 1994) for numerical simulation of electromagnetic wave propagation. Instead of finding an absorbing boundary condition, Berenger found an absorbing boundary layer. An absorbing boundary layer is a layer of artificial absorbing material that is placed to the edges of the grid. The wave is attenuated by the absorption and decays exponentially when it enters the absorbing layer. The PML is considered because of its highly effective, excellent absorption over a wide range of angles and insensitivity to frequency. The PML has been developed for elasticity (Chew and Liu, 1996), poroelasticity (Zeng and Liu, 2001) and anisotropic media (Becache and Joly, 2001). Berenger's original formulation is called a split-field PML, because it splits the variables into two independent parts in the PML region. A later formulation that has become more popular because of its simplicity and efficiency is called uniaxial PML (UPML) which expresses the PML region as the ordinary wave equation with a combination of artificial anisotropic absorbing materials. In this paper, we consider a 2-D visco acoustic medium unsplit-field PML formulation. We describe the PML for viscoacoustic medium and give numerical results using test simulations.

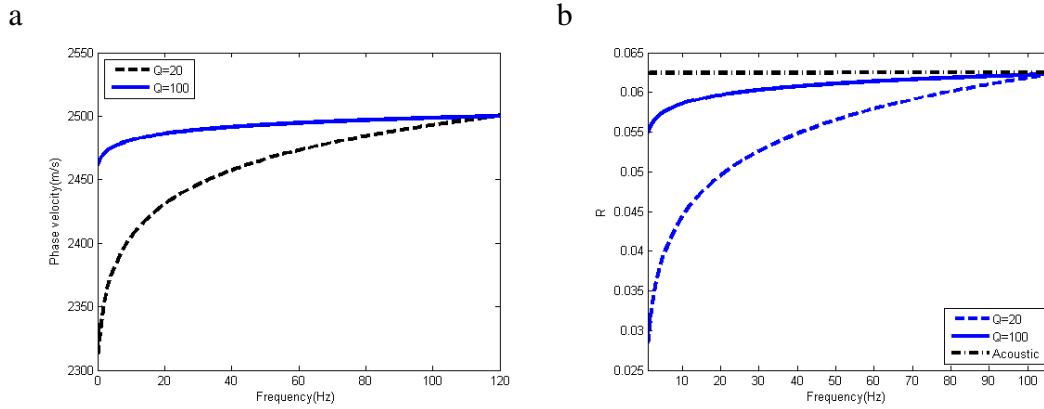


FIG. 1. Illustrate the frequency-dependence of viscoacoustic a) phase velocity and b) reflection coefficient $R(f)$ for different value of Q ($Q = 20$ and $Q = 100$).

ABSORPTION AND ATTENUATION THE MEDIA

To describe the wave propagation in the reflection seismology, acoustic or elastic wave equation is commonly used. The main assumption is that the seismic wave propagates in the heat-insulation media, i.e, it will continue infinitely without the attenuation. However, the Earth is generally anelastic in nature and due to internal friction, seismic waves lose energy as they propagate. The attenuation of seismic waves is due to three effects: geometric spreading, intrinsic attenuation, and scattering. Intrinsic (viscoelastic) attenuation is energy lost to heat and internal friction during the passage of an elastic wave. Seismic attenuation is commonly characterized by the quality factor Q . Attenuation is defined as the ratio of maximum amplitude of a wave field for a particular frequency to the change of amplitude per cycle. By this definition, Q and the attenuation coefficient are related by

$$\alpha(\omega) = \frac{\omega}{2c_0Q} \quad (1)$$

where c_0 is the propagation velocity. Aki and Richards (Aki and Richards, 2002) note that many approaches result in combined absorption and dispersion pairs that, in the context of Q , and on a reasonable seismic frequency band, amount to the replacement of the wavenumber $k = \omega/c_0$ by

$$K = \frac{\omega}{c_0} \left[1 + \frac{i}{2Q} - \frac{1}{\pi Q} \ln\left(\frac{\omega}{\omega_r}\right) \right] \quad (2)$$

where ω_r is a reference frequency, at which the wave field propagates with the phase velocity c_0 . The complex velocity of the constant- Q model can be obtain as

$$v(\omega) = \frac{\omega}{K} = c_0 \left[1 + \frac{i}{2Q} - \frac{1}{\pi Q} \ln\left(\frac{\omega}{\omega_r}\right) \right]^{-1} \quad (3)$$

The real part of complex velocity is attenuated phase velocity and can be written as

$$v_p(\omega) = c_0 \left[1 + \frac{1}{\pi Q} \ln\left(\frac{\omega}{\omega_r}\right) \right] \quad (4)$$

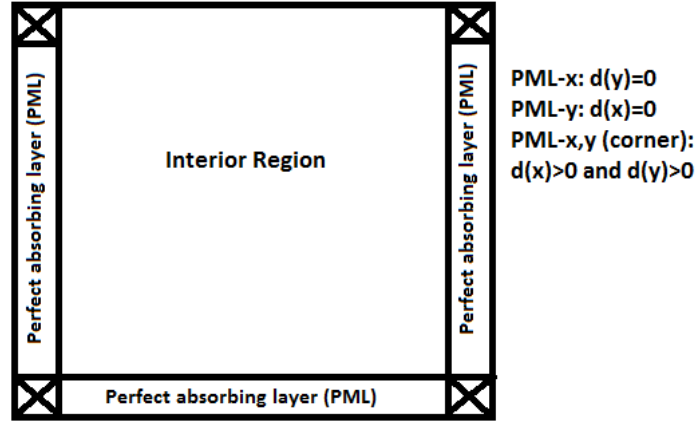


FIG. 2. Illustrate an absorbing layer is placed adjacent to the edges of the computational region—a perfect absorbing layer would absorb outgoing waves without reflections from the edge of the absorber. There are three different PML absorbing regions, PML for x direction ($d(y) = 0$), PML for y direction ($d(x) = 0$), and PML in the corners, both damping parameters $d(x)$ and $d(z)$ are positive, and either $d(z) = 0$ or $d(x) = 0$ inside the PML region in the x and z directions.

where c_0 refer to the reference phase velocity at a reference frequency ω_0 (it usually refers to the phase velocity at the Nyquist frequency). Also the reflection coefficient of viscoacoustic media is complex and frequency dependent and can be written as function of scattering potential (Fathalian and Innanen, 2015).

$$R_{va}(z, \sigma, k) \simeq \frac{i\omega}{2c_0 \cos \theta_0} (\alpha(z) - 2\zeta(z)F(k) + \beta(z)(1 + \cos \sigma)) \quad (5)$$

To understand attenuation effects, we consider a numerical example to describe the phase velocity and reflection coefficient. For a constant Q -model, the attenuation coefficient is linear with frequency ω , while the phase velocity v_p is slightly dependent on frequency. Figure 1 shows how the reflection coefficient and phase velocity are distorted for different Q values for different frequencies. The phase velocity dispersion is more significant when the quality factor is small ($Q=20$), while for $Q=100$ the phase dispersion is much weaker (see Fig. 1a). For a same quality factor Q , the phase delay is more in the lower frequency. The spectra of reflection coefficients for a variety of Q values is illustrated in Figure 1b. The attenuative reflection coefficient approaches its acoustic counterpart as $k \rightarrow k_r$; the variability of R with f increases away from the reference frequency.

FORMULATION

The PML absorbing layer is a non-physical region located outside the artificial numerical boundary as shown in Figure 2. The 2D visco-acoustic medium can be expressed as a system of first-order differential equations in terms of the particle velocities and stresses.

Newton's second law completes the full description of wave propagation in a viscoa-

coustic medium. This is

$$\begin{aligned}\frac{\partial u_x}{\partial t} &= -\frac{1}{\rho} \frac{\partial p}{\partial x} \\ \frac{\partial u_z}{\partial t} &= -\frac{1}{\rho} \frac{\partial p}{\partial z}\end{aligned}\quad (6)$$

where $u(x; t)$ is the particle velocity components in the x and z -direction, $p(x; t)$ is the stress tensor, and $\rho(x)$ is density. The first-order differential equations in terms of the particle velocities and stresses for the 1-D case where the viscoelastic equations are the same as the viscoacoustic can be written as (Robertsson et al., 1994):

$$\frac{\partial p}{\partial t} = -\rho c_p^2 \left(\frac{\partial u_x}{\partial x} + \frac{\partial u_z}{\partial z} \right) \left(1 - \sum_{\ell=1}^L \left(1 - \frac{\tau_{\varepsilon\ell}}{\tau_{\sigma\ell}} \right) \right) - \sum_{\ell=1}^L r_\ell \quad (7)$$

where $\tau_{\varepsilon\ell}$ and $\tau_{\sigma\ell}$ are the stress and strain relaxation times of the ℓ th mechanism and r_ℓ is called memory variables (Carcions et al., 1988a).

$$\frac{\partial r_\ell}{\partial t} = -\frac{1}{\tau_{\sigma\ell}} r_\ell + \rho c_p^2 \left(\frac{\partial u_x}{\partial x} + \frac{\partial u_z}{\partial z} \right) \frac{1}{\tau_{\sigma\ell}} \left(1 - \frac{\tau_{\varepsilon\ell}}{\tau_{\sigma\ell}} \right), 1 \leq \ell \leq L \quad (8)$$

For one memory variable, $L = 1$, the first-order linear differential equations (Eqs. 7 and 8) of viscoacoustic wave propagation are become

$$\frac{\partial p}{\partial t} = -\rho c_p^2 \left(\frac{\partial u_x}{\partial x} + \frac{\partial u_z}{\partial z} \right) \left(\frac{\tau_\varepsilon}{\tau_\sigma} \right) - r \quad (9)$$

$$\frac{\partial r}{\partial t} = -\frac{1}{\tau_\sigma} r + \rho c_p^2 \left(\frac{\partial u_x}{\partial x} + \frac{\partial u_z}{\partial z} \right) \frac{1}{\tau_\sigma} \left(1 - \frac{\tau_\varepsilon}{\tau_\sigma} \right) \quad (10)$$

In order to introduce the PML for visco-acoustic wave, the first-order linear differential equations will be modified using the a complex coordinate stretching approach (Chew and Liu, 1996; Zeng and Liu, 2001; Liu and Tao, 1997). In the frequency domain, the PML formulations can be derived as

$$\begin{aligned}\partial x &\rightarrow \left(1 + \frac{id(x)}{\omega} \right) \partial x \\ \partial z &\rightarrow \left(1 + \frac{id(z)}{\omega} \right) \partial z\end{aligned}\quad (11)$$

where $d(x)$ and $d(z)$ refer to the exponential damping coefficients in the PML region and ω is the temporal frequency. By applying the complex coordinate stretching expressed to the linearized equation of motion and equation of deformation the frequency domain we have

$$\frac{\partial}{\partial t} \left(1 + \frac{id(x)}{\omega} \right) \tilde{u}_x = -\frac{1}{\rho} \frac{\partial \tilde{p}}{\partial x} \rightarrow -i\omega \left(1 + \frac{id(x)}{\omega} \right) \tilde{u}_x = -\frac{1}{\rho} \frac{\partial \tilde{p}}{\partial x} \quad (12)$$

$$\begin{aligned} \frac{\partial}{\partial t} \left(1 + \frac{id(z)}{\omega}\right) \tilde{u}_z &= -\frac{1}{\rho} \frac{\partial \tilde{p}}{\partial z} \rightarrow -i\omega \left(1 + \frac{id(z)}{\omega}\right) \tilde{u}_z = -\frac{1}{\rho} \frac{\partial \tilde{p}}{\partial z} \\ -i\omega \left(1 + \frac{id(x)}{\omega}\right) \left(1 + \frac{id(z)}{\omega}\right) \tilde{p} &= -\rho c_p^2 \left[\left(1 + \frac{id(x)}{\omega}\right) \frac{\partial \tilde{u}_x}{\partial x} + \left(1 + \frac{id(z)}{\omega}\right) \frac{\partial \tilde{u}_z}{\partial z} \right] \left(\frac{\tau_\varepsilon}{\tau_\sigma}\right) - r \\ -i\omega \left(1 + \frac{id(x)}{\omega}\right) \left(1 + \frac{id(z)}{\omega}\right) \tilde{r} &= -\frac{1}{\tau_\sigma} r + \rho c_p^2 \left[\left(1 + \frac{id(x)}{\omega}\right) \frac{\partial \tilde{u}_x}{\partial x} + \left(1 + \frac{id(z)}{\omega}\right) \frac{\partial \tilde{u}_z}{\partial z} \right] \frac{1}{\tau_\sigma} \left(1 - \frac{\tau_\varepsilon}{\tau_\sigma}\right) \end{aligned}$$

To calculate the unsplit-field PML formulations these equations must be transformed back to time domain. So we have

$$\frac{\partial u_x}{\partial t} = -\frac{1}{\rho} \frac{\partial p}{\partial x} - d(x)u_x \quad (13)$$

$$\frac{\partial u_z}{\partial t} = -\frac{1}{\rho} \frac{\partial p}{\partial z} - d(z)u_z$$

$$\frac{\partial p}{\partial t} = -\rho c_p^2 \left(\frac{\partial(u_x + d(z)\mathbf{u}_x)}{\partial x} + \frac{\partial(u_z + d(x)\mathbf{u}_z)}{\partial z} \right) \left(\frac{\tau_\varepsilon}{\tau_\sigma}\right) - (d(x) + d(z))p - d(x)d(z)\mathbf{p} - r$$

$$\frac{\partial r}{\partial t} = -\frac{1}{\tau_\sigma} r + \rho c_p^2 \left[\frac{\partial(u_x + d(z)\mathbf{u}_x)}{\partial x} + \frac{\partial(u_z + d(x)\mathbf{u}_z)}{\partial z} \right] \frac{1}{\tau_\sigma} \left(1 - \frac{\tau_\varepsilon}{\tau_\sigma}\right) - (d(x) + d(z))r - d(x)d(z)\mathbf{r}$$

where the auxiliary variables \mathbf{u}_x , \mathbf{u}_z , \mathbf{p} , and \mathbf{r} are the time-integrated components for velocity, pressure and memory variable fields. They are defined as

$$\mathbf{u}_x(X, t) = \int_{-\infty}^t u_x(X, t') dt' \quad (14)$$

$$\mathbf{u}_z(X, t) = \int_{-\infty}^t u_z(X, t') dt' \quad (15)$$

$$\mathbf{p}(X, t) = \int_{-\infty}^t p(X, t') dt'$$

$$\mathbf{r}(X, t) = \int_{-\infty}^t r(X, t') dt'$$

The relaxation parameters τ_ε and τ_σ are defined as (Robertsson et al., 1994):

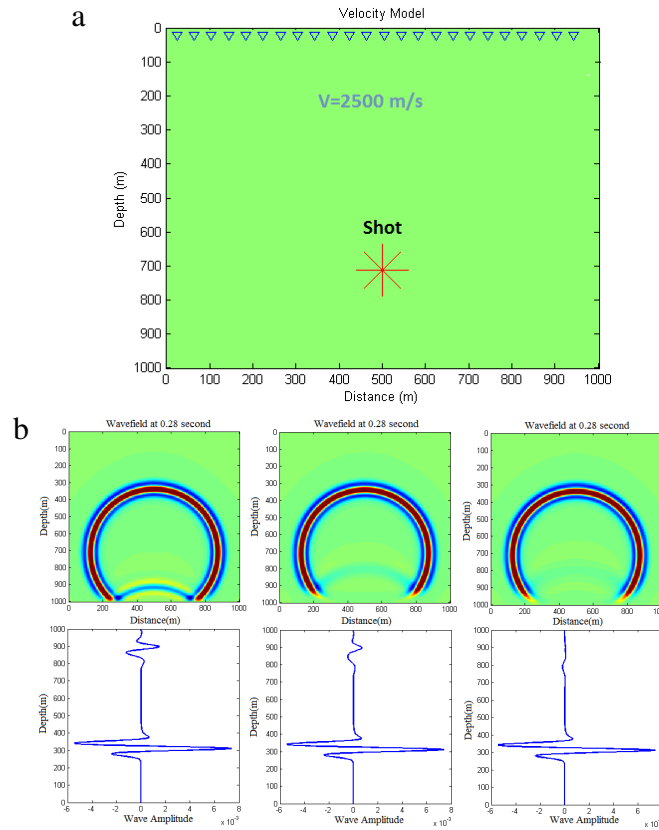


FIG. 3. Illustrate a)The velocity model, b)Snapshots of 2-D viscoacoustic simulations and using the PML absorbing layer model with $\delta = 20m$, $\delta = 40m$, and $\delta = 80m$. The snapshots are the norm of the velocity at $t = 0.28s$.

$$\tau_{\sigma} = \frac{\sqrt{1 + 1/Q.^2} - 1/Q}{f_0} \quad (16)$$

$$\tau_{\epsilon} = \frac{1}{f_0.^2 \tau_{\sigma}} \quad (17)$$

where f_0 is the central frequency wavelet.

There are various unsplit-field PML formulations (Abarbanel and Gottlieb, 1997; Sacks et al., 1995; Turkel and Yefet, 1988; Fan and Liu, 2001; Zhou, 2005) as well-posed which are based on the uniaxial PML and the complex coordinate stretching methods. A simple and systematic method to derive the well-posed PML formulations are useful to apply the PML methods to more complex media. Fan and Liu (Fan and Liu, 2003) proposed the unsplit-field PML formulations, well-posed PML in Cartesian coordinate, for the acoustic wave equations in a lossy medium. In this work, we propose the unsplit-field, strongly well-posed PML for visco acoustic media in Cartesian coordinate. Such a method is very straightforward

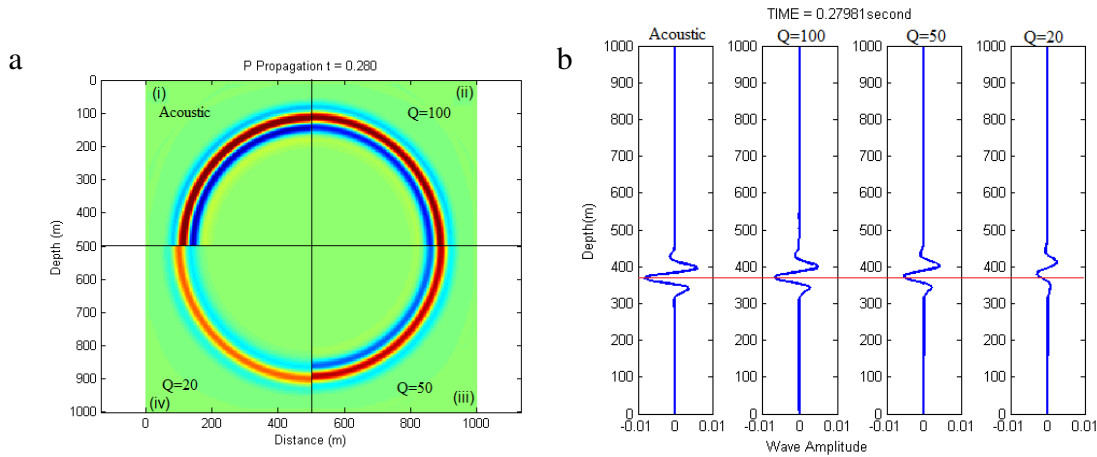


FIG. 4. Illustrate the separation of velocity dispersion (a) and amplitude loss effects(b) at the same simulation configuration. i) Acoustic wavefield, ii) viscoacoustic wavefiled ($Q=100$), iii) viscoacoustic wavefiled ($Q=50$), and iv) viscoacoustic wavefiled ($Q=20$). The value of $v = 2500m/s$ and $\rho = 1200g/m.^3$.

NUMERICAL RESULTS

A perfectly matched layer (PML) is an artificial absorbing layer for wave equations, commonly used to truncate computational regions in numerical methods to simulate problems with open boundaries, especially in the finite-difference (FD) method. In the PML region the outgoing waves from the interior of a computational region strongly absorbed without reflecting them back into the interior while in the inner region, the PML equations are the same as the original wave equations. In the absorbing layers, Collino and Tsogka (Collino and Tsogka, 2001) have used the following model for the damping parameter $d(x)$ that shows a relation based on a theoretical reflection coefficient,

$$d(x) = d_0 \left(\frac{x}{\delta} \right)^2 \quad (18)$$

where δ is the width of the PML layer and d_0 is the maximum damping parameter which is a function of the theoretical reflection coefficient

$$d_0 = \log\left(\frac{1}{R}\right) \frac{3Vp}{2\delta} \quad (19)$$

To investigate the accuracy of solution of the constant- Q wave equation using the PML absorbing boundary condition we consider the constant velocity model. The viscoacoustic medium considered here is characterized by the constant velocity model presented in Figure 3a. The size of the grid is 250×250 , and the source is located at point (500 m, 12 m), which is a zero-phase Ricker wavelet with a centre frequency of 30 Hz. The grid spacing in the x and z directions is 4 m. To reduce artificial reflections that are introduced by the edge of the computational grid, a PML absorbing boundary condition is applied to the sides and bottom of the model. Figure 3b show the snapshots of 2D viscoacoustic wavefiled using the PML absorbing layers. Equations (18) and (19) are used for different width of the PML layer = 20m (5 grid), =40m(10 grid), and =80m ((20 grid)). The theoretical reflection

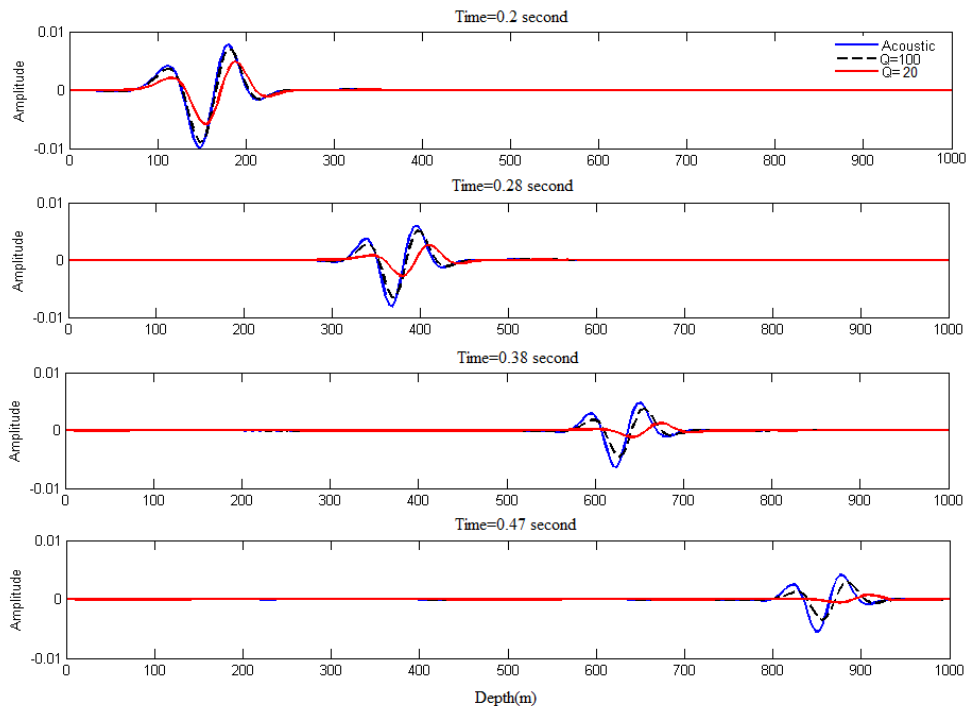


FIG. 5. show depth traces at four different time steps. The solid blue lines, dashed black lines, and solid red lines represent the acoustic and viscoacoustic wave propagation with $Q=100$ and $Q=20$ respectively. The viscoacoustic waveforms have smaller amplitude and wider spread and shifted phase due to velocity dispersion.

coefficient are related with the PML tickness and are close to the numerical ones when the number of meshes inside the layer is large (Collino and Tsogka, 2001). There is no visible artificial reflections observed in the snapshot when the PML layer size is 20 grid, while in the smaller PML layer thicknesses the artificial reflections are visible. The results show that some of waves approaching the boundaries are adsorbed in the PML layer, so some of the artificial reflections are still visible. By spending the computational grid by the size of the PML, we can remove these artificial reflections. The effectiveness of the PML depends on its size and absorption. Also the time step used in the simulation can affect the effectiveness of the PML. For a small time step, the wave spends more time in the PML layer and more absorbed.

Figure 4a and 4b shows the effect of attenuation on amplitude and phase of a propagating seismic wave in a homogeneous medium with a background velocity of 2500 m/s and for different values of quality factor ($Q=20$, $Q=50$ and $Q=100$). The viscoacoustic wavefield has the reduced amplitude and advanced phase in comparison with the acoustic wavefield.

To understand attenuation effects we simulate the 2D viscoacoustic wave propagation with different values of quality factor ($Q=20$, $Q=100$). Figure 5 shows depth traces extracted at four different time steps. The solid blue lines, dashed lines, and solid red lines represent the acoustic and viscoacoustic wave propagation with $Q=20$ and $Q=100$ respectively. There are two main attenuation effects, reduced amplitude and dispersed phase shift. The phases do not match together, and it becomes worse as depth increases because of velocity dispersion in the attenuating media. As the wave starts propagating, the amplitudes in the acoustic

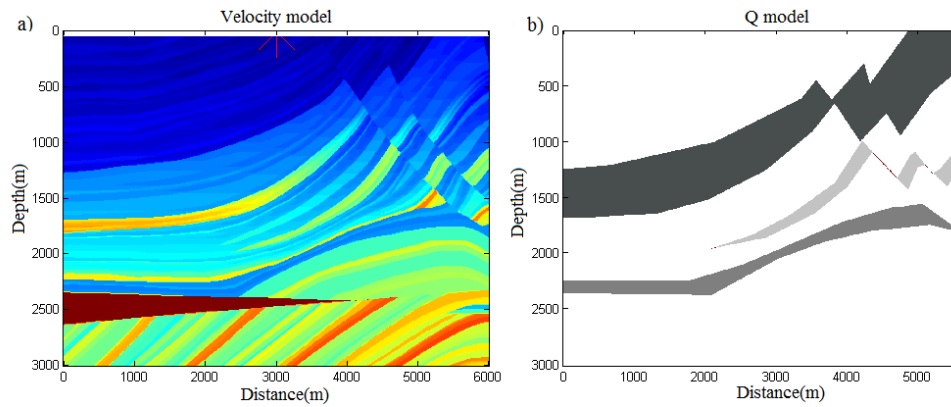


FIG. 6. Illustrate a) Marmousi velocity model, and b) Q model.

and viscoacoustic cases are very similar, while by increasing the propagation time (greater depth), the wave amplitude in case of $Q=20$ is more attenuated. For moderate attenuation values ($Q=100$), as shown by the black dashed curves in Figure 5, the attenuation effect at different depths is still significant compared to the blue curves that represent the acoustic case in which there is no attenuation.

In the second example, we consider the Marmousi model. Figure 6a shows the part of Marmousi velocity model. The model is 6 km wide and 3 km in depth. There is a one shot is located at point (500 m, 12 m), which is a zero-phase Ricker wavelet with a centre frequency of 25 Hz, and receivers are located 4 m apart at 12 m depth. The Q model includes the constant quality factors with different value, while the background of model has $Q = 100$ (Fig. 6b). The FD synthetic data for acoustic and viscoacoustic using equations 6, 9 and 10 are shown in figure 7. The first-order pressure-velocity viscoacoustic wave equation using PML absorbing boundary condition is used to compute the synthetic seismograms. The staggered-grid FD solver has 2nd-order accuracy in time and 4th-order accuracy in space. The snapshots are included the first arrivals, multiples, reflections, refractions and diffractions events. The viscoacoustic simulation have reduced amplitude (particularly multiples) and shifted phase due to velocity dispersion, as highlighted by the red arrow. The

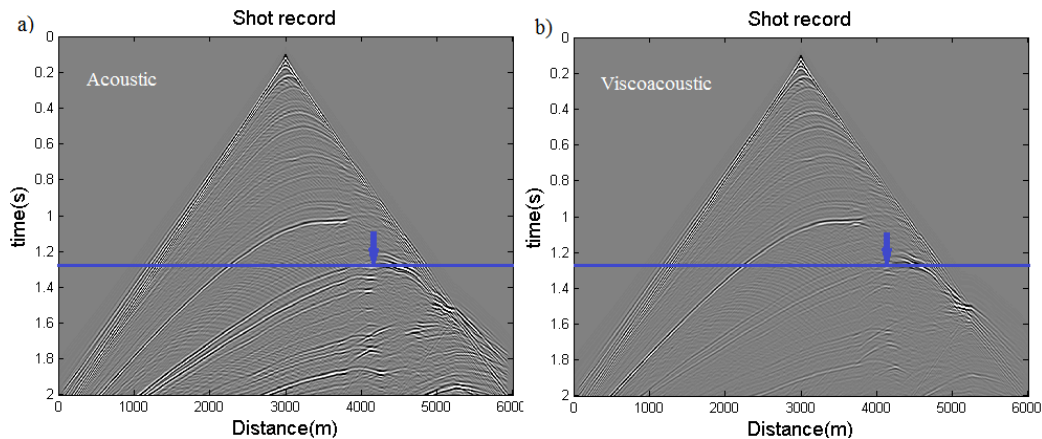


FIG. 7. Show shot record from acoustic simulation (a), and viscoacoustic simulation (b) using PML absorbing boundary condition. Attenuation effects and dispersion of the events highlighted with the blue arrow.

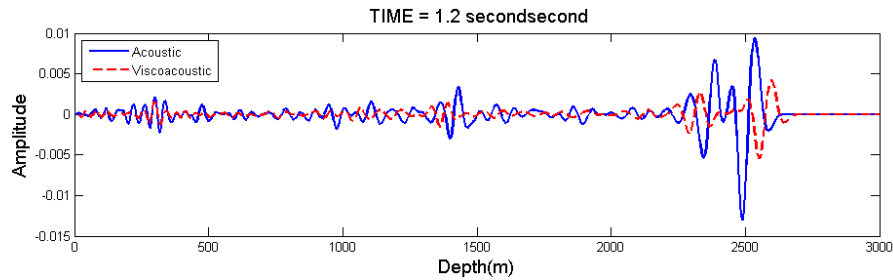


FIG. 8. Illustrate the trace number 900 of acoustic (blue line), and viscoacoustic (red dashed line).

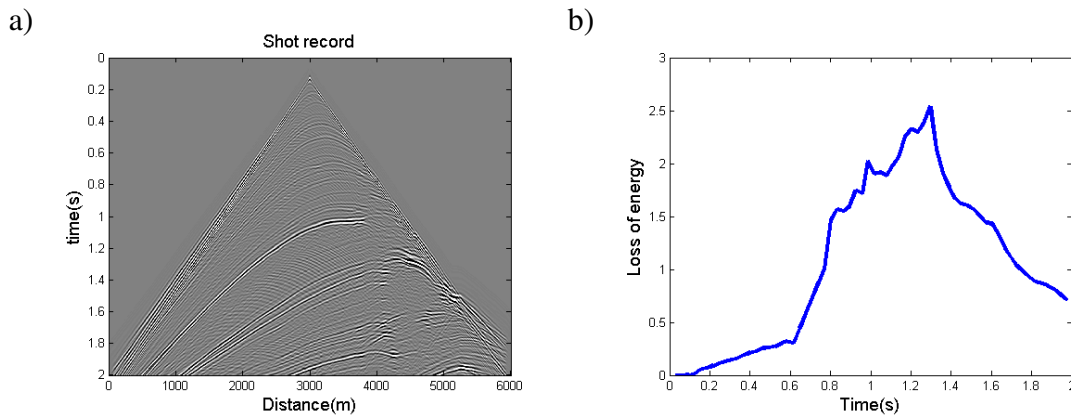


FIG. 9. Illustrate (a) Difference between acoustic and viscoacoustic . (b) The absorption of energy.

trace number 900 of the acoustic and viscoacoustic cases are illustrated in Figure 8, which confirms the reduced amplitude and shifted phase due to attenuation effects. To understand the attenuation effects the difference waveforms between the acoustic and viscoacoustic data are illustrated in Fig. 9a. The energy of waveform is decreased when the wave is propagated in the attenuative media (Fig. 9b).

REVERSE TIME MIGRATION USING UNSPLIT PML VISCOACOUSTIC WAVE EQUATION

The RTM images are computed by the time-space domain FD methods for a layered model with attenuation. The source wavelet is a zero-phase Ricker wavelet with a centre frequency of 25 Hz. The synthetic data are migrated by using acoustic RTM and viscoacoustic RTM. Perfectly matched layer (PML) absorbing boundary conditions are used to attenuate the reflections of an artificial boundary.

A layered model is shown in Fig. 10a with the Q anomaly (Fig. 10b). The model grid measures are 301×401 , the grid size is $4 \text{ m} \times 4 \text{ m}$, the quality factors for background and anomaly (red) are 100 and 20 respectively. The sampling interval is 0.4 ms and the recording length is 2 s.

Figure 11a and 11b compares the RTM images for acoustic and viscoacoustic approximations with the attenuation. The acoustic RTM image has similar artifacts and amplitudes in the shallow layers compared with the viscoacoustic RTM image, while the acoustic RTM image has very weak amplitudes at the deeper layers specially blew the layers with the strong attenuation (blue arrows in Figure 11). This is because strong attenuation affects the amplitudes and the phases of the propagating waves. However, for viscoacoustic RTM the migration amplitudes of layers are more accurate than the acoustic RTM and the reflectors are imaged at the correct locations.

To eliminate source signatures and low-frequency noises we used the imaging condition and highpass filter respectively (Fig. 12). Imaging conditions are used to correlate the source and receiver wavefield snapshots to get the subsurface images. Similar to the acoustic case (Whitmore and Lines, 1986), imaging conditions can be developed for the 2D viscoacoustic case. The imaging conditions for visco-acoustic case:

$$I(x, z) = \frac{\int_t S(x, z, t)R(x, z, t)}{\int_t S^2(x, z, t)} \quad (20)$$

where, $I(x, z)$ is the migration result of the position (x, z) , $S(x, z, t)$ represents the time-domain forward propagated wavefield from the source and $R(x, z, t)$ represents the time-domain receiver wavefield that is back propagated in reverse time from the receiver. The auto-correlation of source in the right can help to remove the effects of source. Also, by applying the highpass filtering method, the RTM image can filter and remove the effects of low-frequency noises.

CONCLUSIONS

A time-domain constant-Q wave propagation by a series of standard linear solid mechanisms is investigated to compensate for the distortion in amplitudes and phases of seismic waves propagating in strong attenuative layers. Numerical synthetic data illustrated for strong attenuation, the acoustic RTM cannot correct for the attenuation loss, while the unsplit viscoacoustic wave equations can compensate the attenuation loss during the iterations. Comparing the synthetic data results for unsplit viscoacoustic and acoustic RTMs show that the migration amplitudes of layers are more accurate than the acoustic RTM and

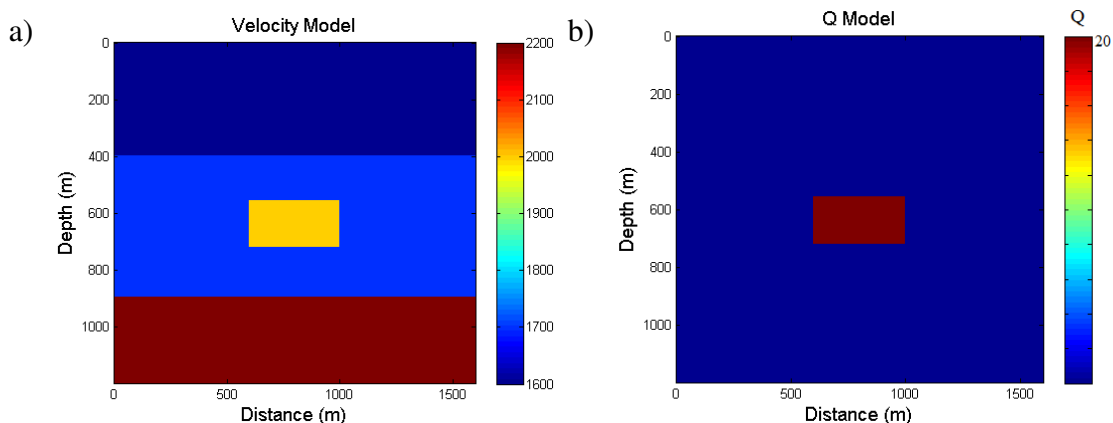


FIG. 10. Illustrate the layered velocity model (a) and Q model (b).

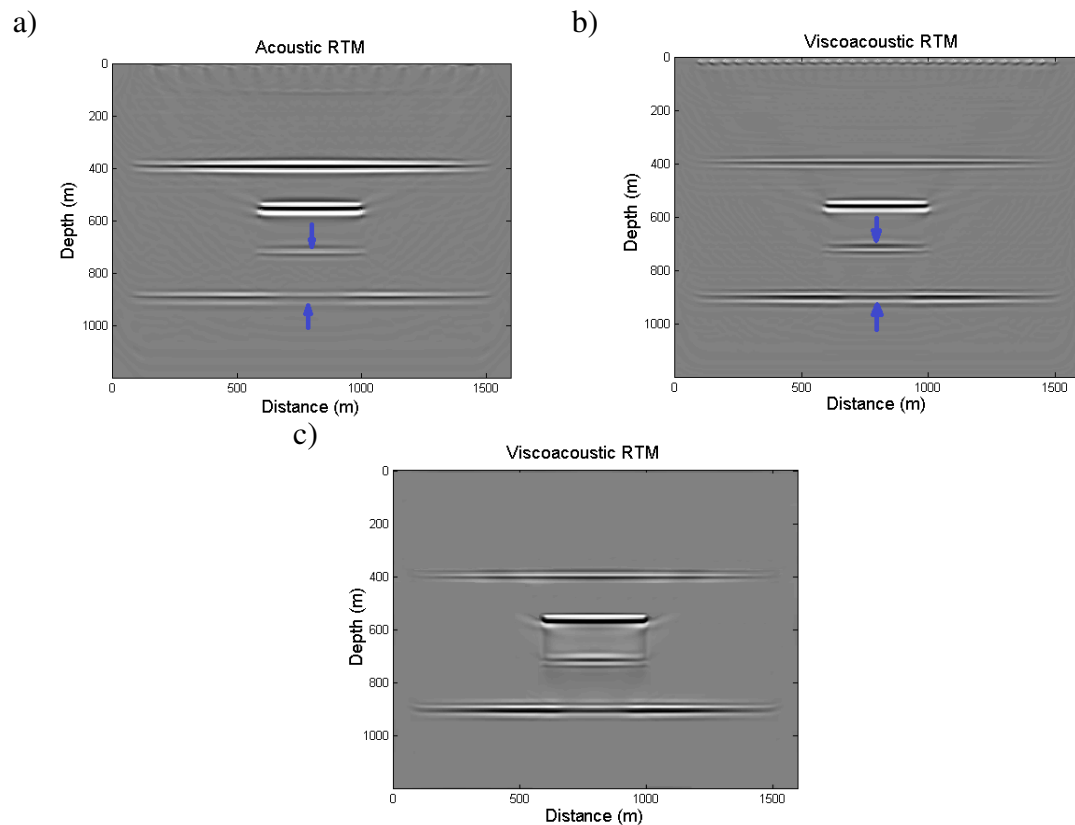


FIG. 11. The RTM images of the layered model (a) acoustic RTM, (b) viscoacoustic RTM, and (c) imaging condition and denoising viscoacoustic RTM. The blue arrows refer to the reflectors below the attenuation layer where we can see that RTM image is clear and the position is accurate from viscoacoustic RTM, compared with the acoustic RTM image.

the reflectors are imaged at the correct locations in strong attenuative media.

ACKNOWLEDGMENTS

The authors thank the sponsors of CREWES for continued support. This work was funded by CREWES industrial sponsors and NSERC (Natural Science and Engineering Research Council of Canada) through the grant CRDPJ 461179-13.

REFERENCES

- Abarbanel, S., and Gottlieb, D., 1997, A mathematical analysis of the pml method: *Jour. Comput. Phys.*, **134**, 357–363.
- Aki, K., and Richards, P. G., 2002, *Quantitative Seismology: USA*: University Science Books.
- Becache, E., and Joly, S. F. P., 2001, Stability of perfectly matched layers, group velocities and anisotropic waves: Tech. Rept. 4304, INRIA.
- Berenger, J., 1994, A perfectly matched layer for the absorption of electromagnetic waves: *Journal of Computational Geophysics*, **114**, 185–200.
- Cerjan, C., Koslo, D., Koslo, R., and Reshef, M., 1985, A non-reflecting boundary condition for direct acoustic and elastic wave equations: *Geophysics*, **50**, 705–708.

- Chew, W., and Liu, Q., 1996, Perfectly matched layers for elastodynamics: a new absorbing boundary condition: *Journal of Computational Acoustics*, **4**, 341–359.
- Clayton, R., and Engquist, B., 1977, Absorbing boundary conditions for acoustic and elastic wave equations: *Bull. Seis. Soc. Am.*, **67**, 1529–1540.
- Collino, F., and Tsogka, C., 2001, Application of the perfectly matched absorbing layer model to the linear elastodynamics problem in anisotropic heterogeneous media: *Geophysics*, **66**, 294–3007.
- Fan, G., and Liu, Q., 2001, A well-posed pml absorbing boundary condition for lossy media: *IEEE Antennas Propagat. Soc. Int. Sym.*, **3**, 2–5.
- Fan, G., and Liu, Q., 2003, A strongly well-posed pml in lossy media: *IEEE ANTENNAS AND WIRELESS PROPAGATION LETTERS*, **2**, 97–100.
- Fathalian, A., and Inananen, K., 2015, Direct nonlinear inversion of viscoacoustic media using the inverse scattering series: *crewees reports 2015*.
- Levander, A. R., 1985, Use of the telegraphy equation to improve absorbing boundary efficiency for fourth-order acoustic wave finite difference schemes: *Bull. Seismol. Soc. Am.*, **75**, 1847–1852.
- Liu, Q., and Tao, J., 1997, The perfectly matched layer (pml) for acoustic waves in absorptive media: *Jour. Acoust. Soc. Am.*, **102**, 2072–2082.
- Robertsson, J. O. A., Blanch, J. O., and Symes, W. W., 1994, Viscoelastic finite-difference modeling: *Geophysics*: *Geophysics*, **59**, 1444–1456.
- Sacks, Z. S., Kingsland, D. M., Lee, R., and Lee, J. F., 1995, A perfectly matched anisotropic absorber for use as an absorbing boundary condition: *IEEE Trans. Antennas and Propagation*, **43**, 1460–1463.
- Turkel, E., and Yefet, A., 1988, Absorbing pml boundary layers for wave-like equations: *Appl. numer. Math.*, **27**, 533–557.
- Whitmore, N., and Lines, L., 1986, Vertical seismic profiling depth migration of a salt-dome flank: *Geophysics*, **51**, 1087–1109.
- Zeng, Y., and Liu, Q., 2001, A staggered-grid finite difference method with perfectly matched layers for poroelastic wave equations: *Jour. Acoust. Soc. Am*, **109**, 2571–2580.
- Zhou, M., 2005, A well-posed pml absorbing boundary condition for 2d acoustic wave equation: *University of Utah*.